ELSEVIER

Polymer 42 (2001) 1227–1241

polymer

www.elsevier.nl/locate/polymer

Crack healing in poly(methyl methacrylate) induced by co-solvent of methanol and ethanol

Hsin-Chan Hsieh[a], Tsong-Jen Yang[b], Sanboh Lee[a,*]

[a]*Department of Materials Science, National Tsing Hua University, Hsinchu 30043, Taiwan, ROC*
[b]*Department of Materials Science, Feng Chia University, Taichung 400, Taiwan, ROC*

Received 6 March 2000; received in revised form 24 May 2000; accepted 26 May 2000

Abstract

The crack healing of poly(methyl methacrylate)(PMMA) treated with a solvent mixture of methanol and ethanol was studied. The mass transport of the solvent mixture in PMMA is anomalous; it is mixed Case I and Case II transport. The data of mass transport can be analyzed by Harmon's model. It was found that the activation energies of Case I and Case II transport of mixture are equal to the summation of the corresponding quantities for methanol and ethanol with each weight factor based on the respective volume fraction. The solubility of the mixture is equal to the summation of solubilities of methanol and ethanol with weighting factor based on their molecular weight. The solvent healing including wetting and diffusion stages was analyzed based on the morphology and mechanical strength. The crack closure rate is constant during the wetting stage. Comparing the activation energies of both mass transport and crack closure rate, the crack tip recession is controlled by Case II transport. Crack tip recession was observed from both lateral and top views. The mechanical strength of the healed specimen increases with decreasing volume fraction of ethanol. Fractography was provided as evidence of recovery of mechanical strength.

Keywords: Crack healing; Poly(methyl methacrylate); Methanol

1. Introduction

Crack healing has been receiving much attention. Jud and Kaush [1] observed that molecular chain diffusion occurs at the treated temperature exceeding the glass transition temperature. Wool and O'Connor [2] studied thermal healing in polymers in terms of five stages: (a) surface rearrangement, (b) surface approach, (c) wetting, (d) diffusion, and (e) randomization. Yu et al. [3] proposed a theory for the constant rate of crack closure during the wetting stage. Kim and Wool [4] proposed a theory of the diffusion and randomization stages based on the reptation model of chain dynamics analyzed by de Gennes [5]. Wool and O'Connor [2], Wool [6], and Voyutskii [7] found that the healed fracture stress is proportional to $t^{1/4}$ for polybutadiene and polyisobutylene, where t is the healing time. Wool [8] described the thermal healing in polymers in detail. In contrast to thermal healing, solvent healing is undertaken at the treated temperature below the glass transition temperature. The solvent is introduced to a polymer until healing and then removed. Solvent healing was observed in poly(methyl methacrylate) (PMMA) using methanol and ethanol [9–11], and in polycarbonate using carbon tetrachloride [12].

Alfrey et al. [13] categorized solvent transport behavior in polymers as the following: (a) Case I (Fickian), (b) Case II, and (c) anomalous. The anomalous behavior is a combination of Case I and Case II transport. Case I transport with different boundary conditions and diffusivities was extensively collected by Crank [14] and his references. The mechanism of Case II behavior was studied by many researchers [15–22]. Kwei and coworkers [23–27] were the first to propose a model to analyze Case I, Case II and anomalous behavior in polymers. Kwei's equation was modified from infinite medium to finite medium by Harmon et al. [28,29]. Harmon's equation was applied successfully to various polymer–solvent systems [8–10,30–32].

According to Cowie et al. [33], a mixture of water and alcohol containing 0.4 volume fraction of water is a good solvent for PMMA at room temperature. Lin et al. [34] found that PMMA treated with a mixture of water containing 0.95 volume fraction ethanol attained the greatest strength of adhesion at 90°C. It was found that PMMA that underwent crack healing by treatment with methanol fully recovered its mechanical strength [9], but not with ethanol treatment [10]. It prompted us to study the co-solvent of methanol and

* Corresponding author. Tel.: +886-3-5719677; fax: +886-3-5722366.
E-mail address: sblee@mse.nthu.edu.tw (S. Lee).

0032-3861/01/$ - see front matter © 2000 Elsevier Science Ltd. All rights reserved.
PII: S0032-3861(00)00407-9

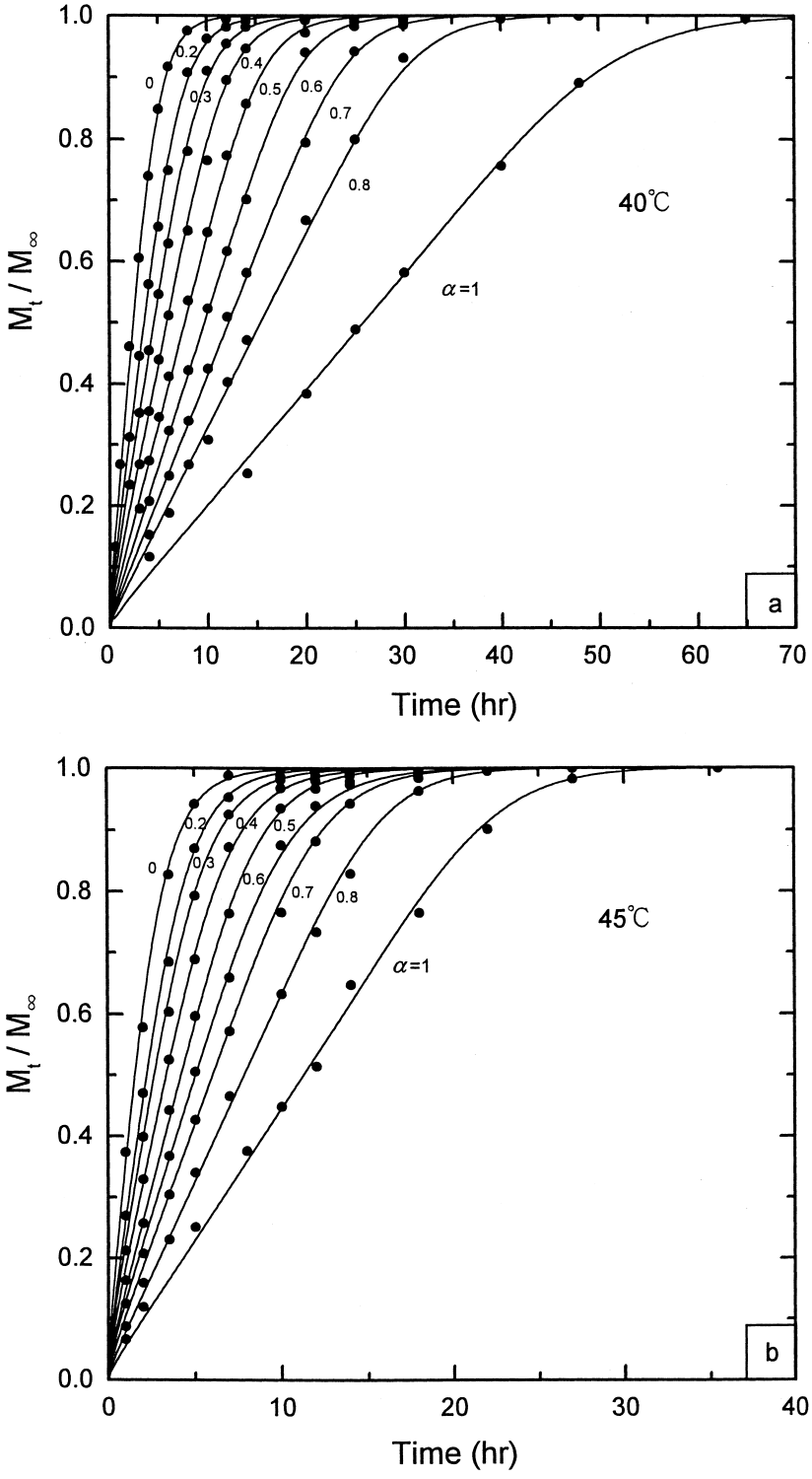

Fig. 1. Co-solvent transport in uncracked PMMA at temperature: (a) 40°C; (b) 45°C; (c) 50°C; (d) 55°C; and (e) 60°C. α represents the volume fraction of ethanol to co-solvent.

ethanol-induced crack healing in PMMA. The next section states the experimental procedure. The third section deals with results and discussion including mass transport, sharp front, crack closure rate, fracture stress of healed specimen, and fractography. Finally, a conclusion was made.

2. Experimental

PMMA with inherent viscosity 0.237 dl/g was obtained from Du Pont in the form of a 6.3 mm thick Lucite L type cast acrylic sheet. Two sizes of sample were cut from the

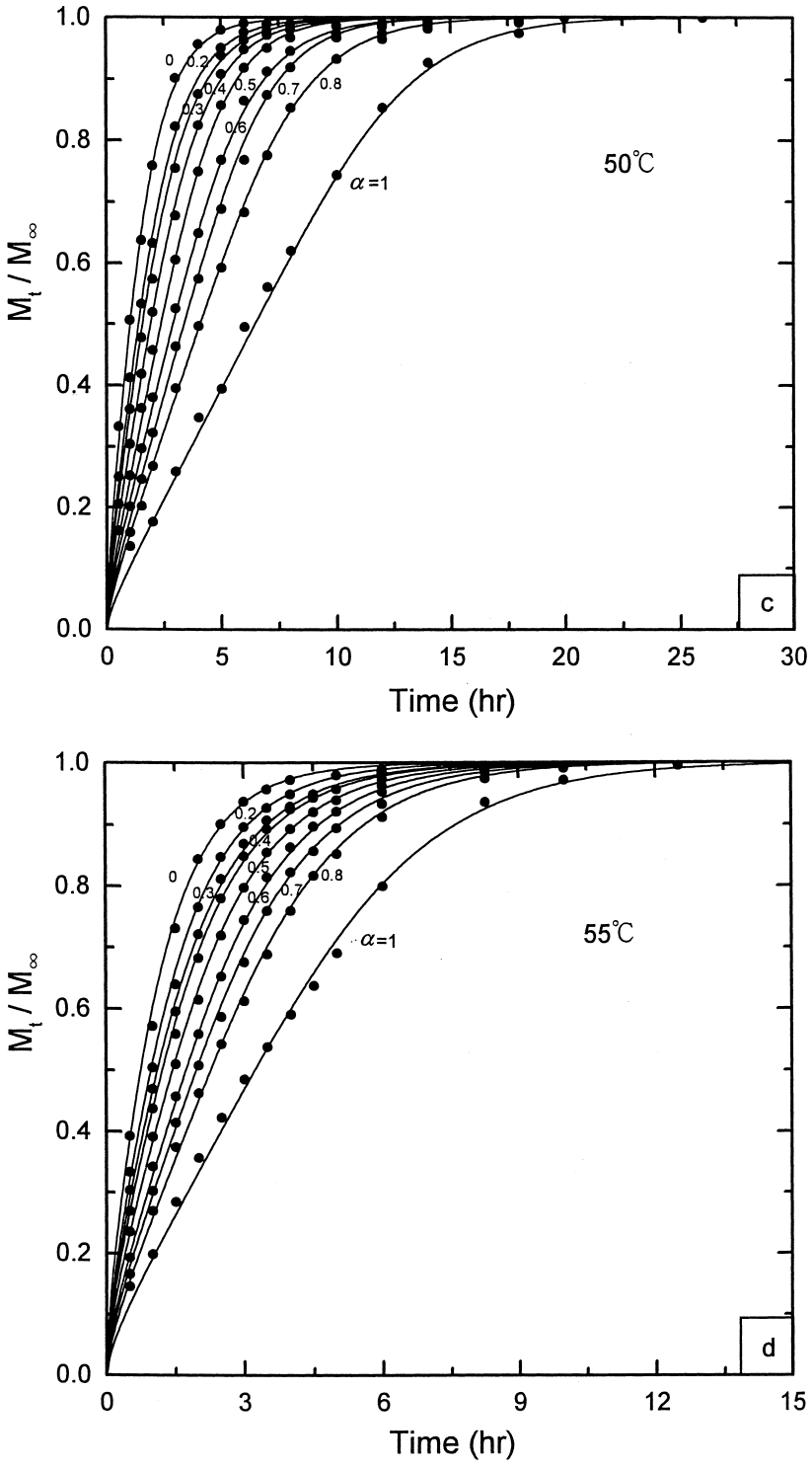

Fig. 1. (*continued*)

sheet. One is the size of $40 \times 6.3 \times 1.0$ mm for mass transport measurement and the other is $80 \times 6.3 \times 1.0$ mm for sharp front and crack healing observations. All samples were ground on 600 and 1000 grid carbimet papers followed by final polishing with 1 μm and 0.3 μm alumina slurries. Then the samples were annealed for 24 h at 120°C in air and furnace-cooled to room temperature. A crack was induced by a sharp blade and propagated until the ligament length was approximately 0.3 mm. The co-solvent is a mixture of methanol and ethanol with various volume ratios. The volume percentages of ethanol in co-solvent are 100,

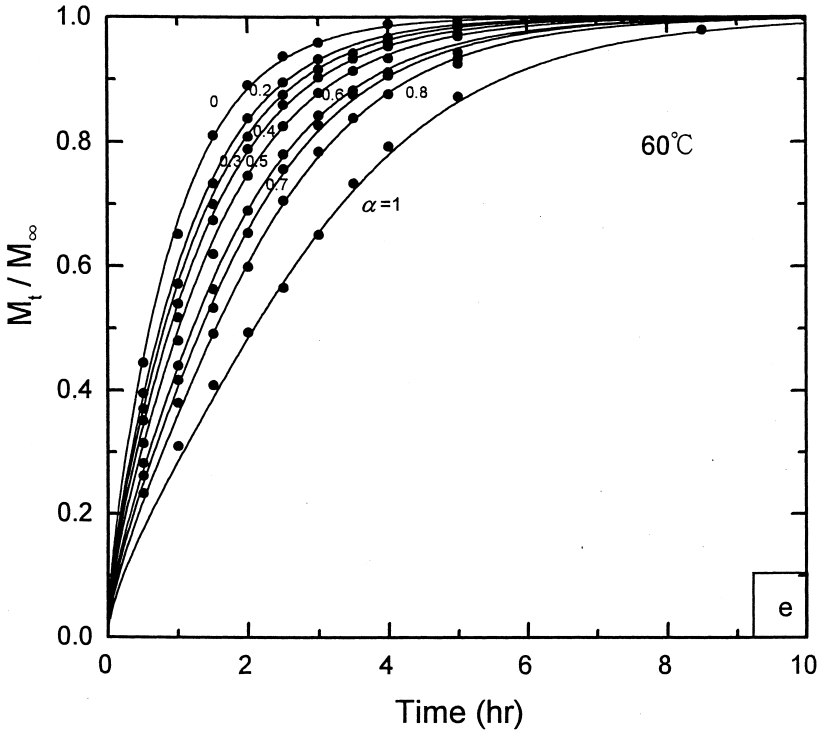

Fig. 1. (*continued*)

80, 70, 60, 50, 40, 30, 20 and 0 (or $\alpha = 1$, 0.8, 0.7, 0.6, 0.5, 0.4, 0.3, 0.2 and 0, respectively).

Uncracked samples for mass transport measurement were preheated to the treated temperature. Each sample was put into the glass bottle filled with co-solvent kept in a thermostat water bath at 40 ~ 60°C. The mass transport was carried out by measuring weight gain of sample periodically. Samples were removed from the glass bottle, blotted, and weighed in a Kern 870 digital balance. Then the sample was returned immediately to the water bath for another period. This process was repeated until saturated.

The process of sharp front observation was similar to the mass transport. Whenever the sample was removed from water bath, a small part of sample was cut to observe the sharp front using an Olympus BH-2 optical microscope. The picture of the sharp front was taken using a Nikon camera and the time was recorded. This process was continued until both sharp fronts met at the center.

Cracked samples were used to observe the crack healing. The cracked sample was immersed in a co-solvent similar to that of mass transport and its crack tip recessed. A set of continuous pictures of crack tip recession was taken using a Nikon camera. The slope of position of crack tip versus time was calculated to give the crack closure rate. Each set of data was obtained from five samples. The healed sample was moved into a vacuum chamber at the same temperature for desorption until it reached equilibrium. Then the sample was machined to remove defects such as the region containing crack initiation and the ligament region before healing. The healed sample was tested by a tensile test machine with a cross-head speed of 0.014 mm/s at room temperature. Data were obtained from three to five samples. We also observed the fractography using the Olympus BH-2 optical microscope.

The effect of co-solvent on glass transition temperature of poly(methyl methacrylate) was studied with a SEIKO I-200 Differential Scanning Calorimeter (DSC). The sample of approximately 10 mg was immersed in co-solvent until saturated at 40 ~ 60°C. After removal from the water bath, the sample was immediately enclosed in a regular aluminum pan and moved into the DSC. The sample was heated from −40 to 100°C with a heating rate of 5°C/min and a nitrogen flow of 40 ml/min. Then it was cooled from 100 to −40°C with a cooling rate of 5°C/min, held at −40°C for 20 min, and then heated again. The heat flow of the system was recorded.

3. Results and discussion

3.1. Mass transport

The data of co-solvent transport in uncracked PMMA are shown in Fig. 1(a)–(e), where α is the volume ratio of ethanol to solvent mixture (or co-solvent). These curves of weight gain versus time can be analyzed by the mass transport model proposed by Harmon et al. [28,29] in which the mass transport is accounted for by Case I, Case II and anomalous diffusion. The characteristics parameters D and v represent Case I and Case II transport, respectively. A

Table 1
D and v for methanol–ethanol transport in PMMA and its solubility S

α	D and v	T (°C)				
		40	45	50	55	60
0	$D\times10^8$ (cm^2/s)	1.2	2.5	4.7	10	20
	$v\times10^6$ (cm/s)	2.7	3.6	4.7	6.1	8
	S (%)	33.7	37.8	42.2	47	53
0.2	$D\times10^8$ (cm^2/s)	0.7	1.2	2.7	5.5	13
	$v\times10^6$ (cm/s)	1.9	2.6	3.55	4.7	6.5
	S (%)	35.2	40.6	45.3	51	58.1
0.3	$D\times10^8$ (cm^2/s)	0.4	0.95	2	4.3	9.5
	$v\times10^6$ (cm/s)	1.4	2.2	3	4	5.5
	S (%)	36.1	41.4	46.5	53.3	61.3
0.4	$D\times10^8$ (cm^2/s)	0.22	0.55	1.2	3.	7
	$v\times10^6$ (cm/s)	1.1	1.7	2.5	3.5	4.8
	S (%)	36.7	42.6	48.1	55.1	64.4
0.5	$D\times10^8$ (cm^2/s)	0.12	0.3	0.7	2	5
	$v\times10^6$ (cm/s)	0.86	1.35	2.1	3	4.2
	S (%)	37.3	43.8	49.7	57.7	66.7
0.6	$D\times10^8$ (cm^2/s)	0.06	0.2	0.5	1.3	3.5
	$v\times10^6$ (cm/s)	0.65	1	1.65	2.6	3.7
	S (%)	38	44.4	51.2	59.6	70.4
0.7	$D\times10^8$ (cm^2/s)	0.037	0.1	0.3	1	2.5
	$v\times10^6$ (cm/s)	0.5	0.8	1.4	2.3	3.3
	S (%)	38.8	45.6	52.9	62.1	74.2
0.8	$D\times10^8$ (cm^2/s)	0.023	0.06	0.2	0.7	1.9
	$v\times10^6$ (cm/s)	0.36	0.7	1.1	2	3
	S (%)	39.5	47	55.3	65.3	78.8
1	$D\times10^8$ (cm^2/s)	0.014	0.03	0.2	0.5	1.5
	$v\times10^6$ (cm/s)	0.22	0.48	0.8	1.6	2.5
	S (%)	42.1	50.5	61.1	73.4	88.7

PMMA plate of thickness 2ℓ is assumed to be solvent-free at the initial time. The concentration at outer boundary surfaces is maintained constant, C_0, for $t \geq 0$, where t is the diffusion time. The fluxes of both Case I and Case II transport are from the outer surface towards the center. According to Harmon et al. [28,35], the weight gain based on one-dimensional model is written as

$$\frac{M_t}{M_\infty} = 1 - 2\sum_{n=1}^{\infty} \frac{\lambda_n^2(1-\cos\lambda_n\, e^{-v\ell/2D})}{\beta_n^4\left(1-\frac{2D}{v\ell}\cos^2\lambda_n\right)}\exp(-\beta_n^2 Dt/\ell^2) \quad (1)$$

where $$\beta_n^2 = \frac{v^2\ell^2}{4D^2} + \lambda_n^2 \quad (2)$$

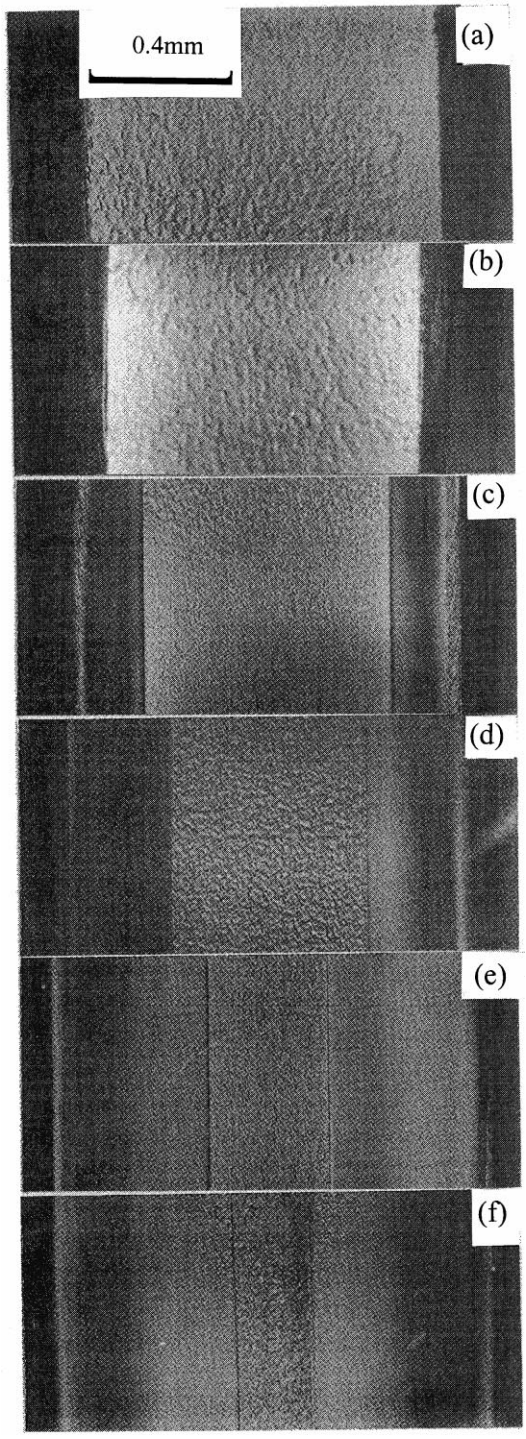

Fig. 2. A set of continuous pictures of sharp front in PMMA with $\alpha = 0.5$ at 50°C for periods of (a) 0 min; (b) 30 min; (c) 60 min; (d) 90 min; (e) 120 min; and (f) 150 min.

Table 2
Activation energies of Case I (E_D) and Case II (E_v) transport, crack closure (E_H), and heat of mixing (ΔH), with various α, where α is the volume ratio of ethanol to mixture

α	0	0.2	0.3	0.4	0.5	0.6	0.7	0.8	1
E_D (kcal/mol.)	29.1	31.8	33.0	35.7	38.8	41.5	44.5	46.8	50.4
E_v (kcal/mol.)	11.2	12.7	13.8	15.2	16.6	18.4	20.1	22.0	25.1
ΔH (kcal/mol.)	−4.6	−5.1	−5.4	−5.7	−6.0	−6.3	−6.6	−7.1	−7.7
E_H (kcal/mol.)	28.7	31.0			38.2			46.3	50.1

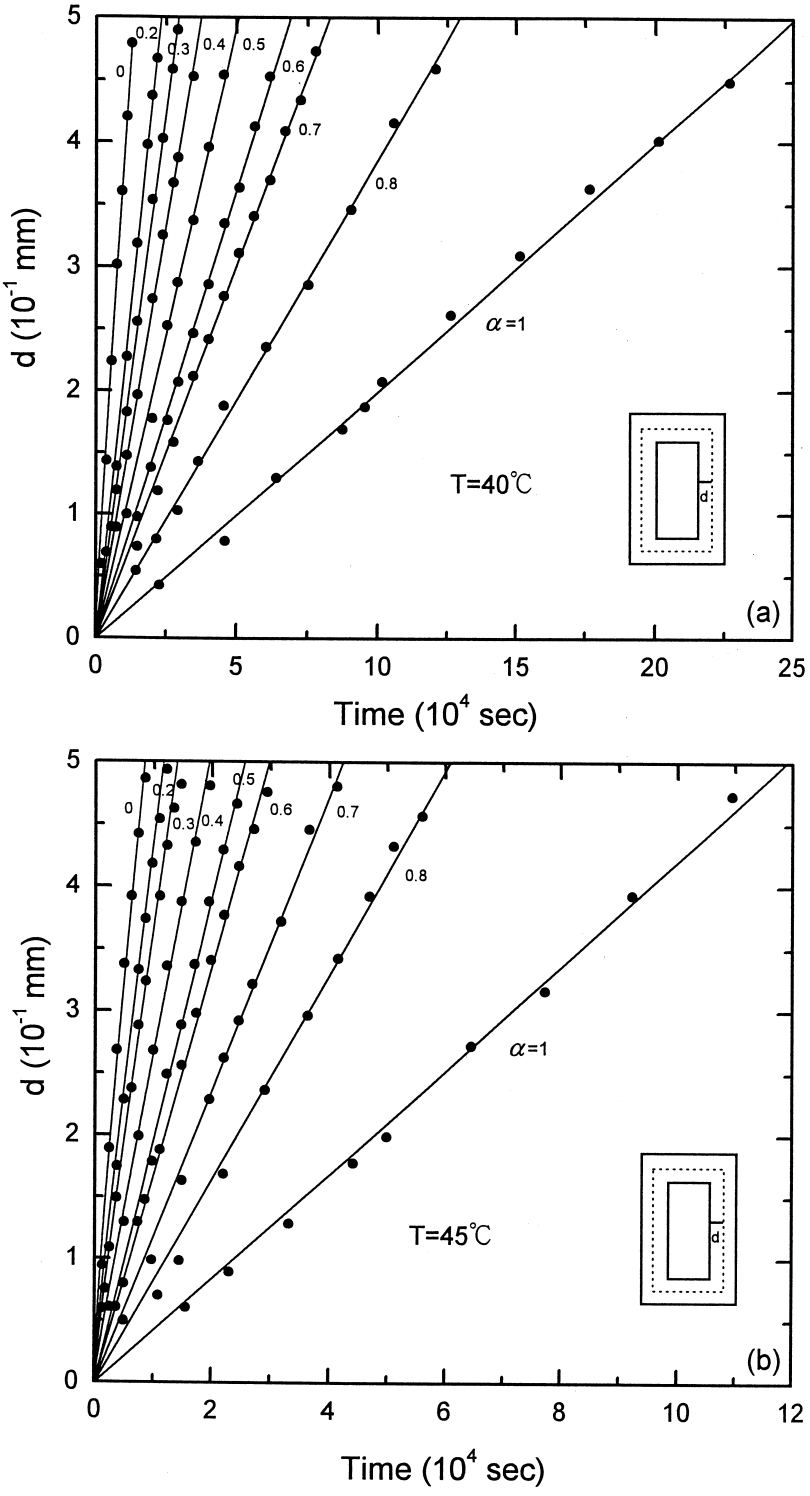

Fig. 3. The displacement d of sharp front as a function of transport time: (a) 40°C; (b) 45°C; (c) 50°C; (d) 55°C; and (e) 60°C. A schematic of the sharp front in the specimen is shown in the inset where the dashed line is the boundary of specimen before solvent treatment. Outer and inner coarse lines stand for the boundary of specimen and the sharp front at time t, respectively.

and λ_n is the positive nth root of the following equation

$$\lambda = \frac{v\ell}{2D}\tan\lambda \tag{3}$$

$M_\infty (= 2\ell AC_0)$ is the weight gain at time infinity and A is the cross-section of specimen. The solid line in Fig. 1 is obtained using Eq. (1) with Eqs. (2) and (3). It can be seen from Fig. 1 that the theory is in good

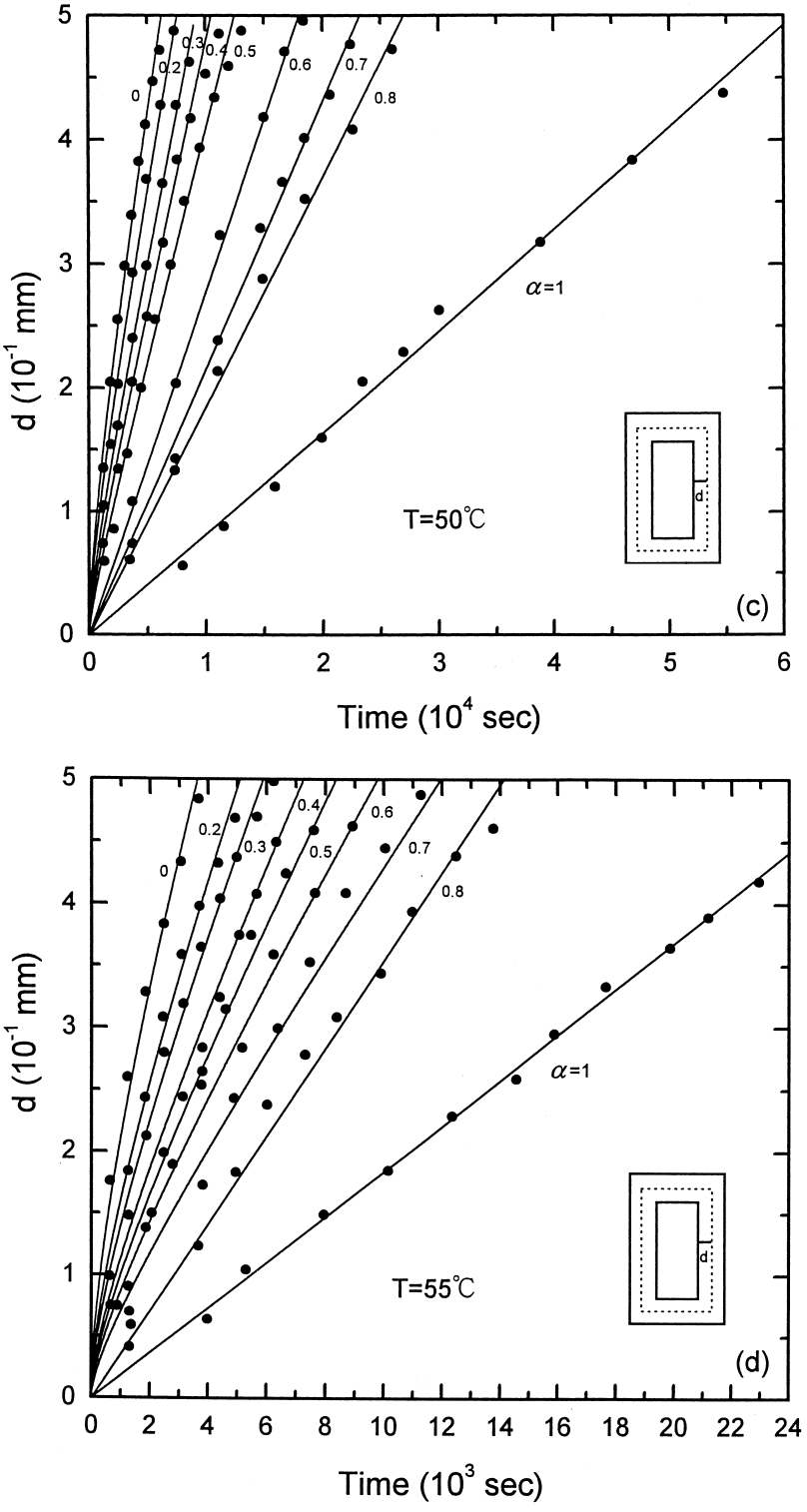

Fig. 3. (*continued*)

agreement with the experimental data. From Fig. (1) with Eq. (1), we obtain the characteristic parameters D and v and list them in Table 1. At the same temperature, both D and v increase with decreasing volume fraction of ethanol. Both D and v obey Arrhenius' equation

$$D = D_0 \exp(-E_D/RT) \tag{4a}$$

$$v = v_0 \exp(-E_v/RT) \tag{4b}$$

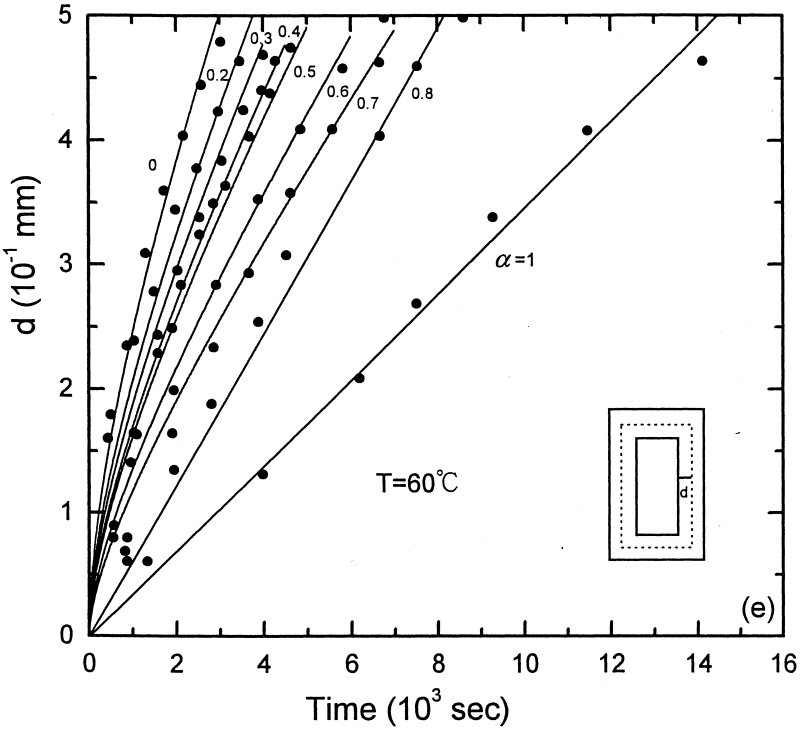

Fig. 3. (*continued*)

where D_0 and v_0 are pre-exponent factors and E_D and E_v are activation energies of Case I and Case II transport, respectively. Using Eq. (4) with Table 1, the activation energies of Case I (E_D) and Case II (E_v) are calculated and listed in Table 2. It is found that E_D and E_v increase linearly with the volume fraction of ethanol. That is, the activation energies of Case I and Case II transport of mixture are equal to the summation of their corresponding quantities with weighting factor based on the volume fraction. This indicates that during the mass uptake, ethanol does not interact with methanol. They transport separately in the PMMA specimen.

The solubility S is defined as mass of saturated co-solvent in the specimen divided by mass of specimen before solvent uptake. The solubility as a function of temperature and volume fraction of ethanol to mixture is listed in Table 1. For a given temperature, the solubility increases parabolically with volume fraction of ethanol. The molecular weight of mixture also increases parabolically with volume fraction of ethanol. Thus the solubility increases linearly with molecular weight of solvent mixture. For a given fraction of ethanol, the solubility satisfies van't Hoff's equation

$$S = S_0 \exp(\Delta H/\mathrm{R}T) \tag{5}$$

where S_0 and ΔH are pre-exponent factor and heat of mixing, respectively. Using Eq. (5) with Table 1, we calculate the heat of mixing and list in Table 2. The negative sign of ΔH in Table 2 indicates that the mass transport in PMMA is an exothermic process. The heat of mixing (absolute value) increases linearly with increasing volume fraction of ethanol to mixture. Again this is evidence that methanol and ethanol diffuse separately in the PMMA specimen.

3.2. Sharp front

The sharp front, which separates the swollen zone from the glassy core, was observed in the PMMA/methanol–ethanol co-solvent system. Fig. 2 shows a set of continuous pictures of sharp fronts in the PMMA with $\alpha = 0.5$ at 50°C. The time interval between two successive pictures is 30 min. The displacement of the sharp front is a function of time as shown in Fig. 3. It is found that both sharp fronts meet at the center before the solvent saturates. The displacement d of sharp front shown in Fig. 3 can be curve-fitted by the following

$$d = at^{0.5} + bt, \tag{6}$$

where a and b are constants. Case I and Case II diffusion affect the first and second terms in Eq. (6), respectively. Using Eq. (5) with Fig. 3, the coefficients a and b are calculated and listed in Table 3. It can be seen from Table 3 that both a and b increase with increasing temperature and volume fraction of ethanol. The coefficients a and b satisfy Arrhenius' equation. The activation energies of a and b are calculated and listed in Table 4. The activation energy of E_a increases with increasing volume fraction of ethanol until it becomes stable at $\alpha = 0.5$ When α is greater than 0.6, Case II transport dominates. Both activation energies of a and b are smaller than those of Case I and Case II transport in a given PMMA/methanol–ethanol system, respectively.

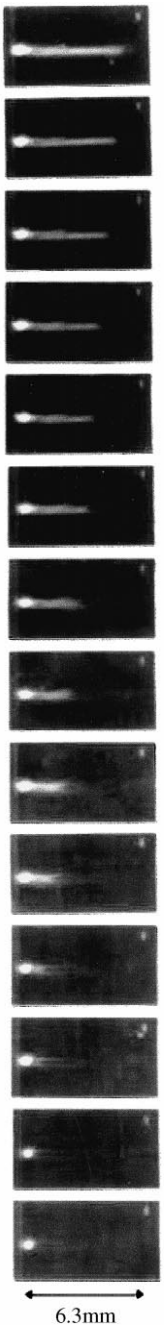

Fig. 4. A set of continuous pictures of crack healing in PMMA treated by mixture of $\alpha = 0.5$ The time interval between two successive pictures is 30 s.

The sharp front is due to the change of optical density from the swollen region to the glassy core. The optical density is affected by the microstructure. The optical density of the rubber state is different from that of the glassy state. When PMMA is immersed in the mixture of methanol–ethanol, the glass transition temperature of PMMA lowers. As soon as the effective glass transition temperature of specimen treated with solvent is greater than the glass transition temperature, the specimen changes from the glassy to the rubber state. The swollen zone is in the rubber state. Furthermore, the swollen PMMA has a lower refractive index n than does dry glassy PMMA ($n = 1.5$). This is because methanol has a low refractive index (about 1.33). The change of optical density is more pronounced for glass-to-liquid transition than for glass-to-rubber transition. Thus the optical density of the swollen zone is different from that of the glassy core. In summary, the major mechanism of sharp front is glass-to-liquid transition.

Table 3
The values of a and b for various volume ratios α of ethanol to mixture and transport temperature T

α	a and b	T (°C)				
		40	45	50	55	60
0	$a \times 10^4$ (cm^2/s)	0.9	2	2.8	5	6
	$b \times 10^6$ (cm/s)	3	3.8	4.5	5.5	5.8
0.2	$a \times 10^4$ (cm^2/s)	–	1.1	2.2	3.6	4.9
	$b \times 10^6$ (cm/s)	2.17	3.3	4.1	4.8	5.3
0.3	$a \times 10^4$ (cm^2/s)	–	0.7	1.5	3	4.4
	$b \times 10^6$ (cm/s)	1.71	3	3.9	4.6	5
0.4	$a \times 10^4$ (cm^2/s)	–	03.8	1.1	2.3	3.9
	$b \times 10^6$ (cm/s)	1.34	2.3	3.7	4.2	4.8
0.5	$a \times 10^4$ (cm^2/s)	–	–	0.8	2	3.7
	$b \times 10^6$ (cm/s)	0.99	1.96	3.3	3.8	4.6
0.6	$a \times 10^4$ (cm^2/s)	–	–	–	1.7	3
	$b \times 10^6$ (cm/s)	0.72	1.68	2.78	3.4	4.2
0.7	$a \times 10^4$ (cm^2/s)	–	–	–	1.3	2.5
	$b \times 10^6$ (cm/s)	0.60	1.18	2.16	3	4

3.3. Crack closure rate

The cracked specimen with ligament length of 0.3 mm is healed in the mixture of methanol and ethanol in the range of 40–60°C without any external force. Crack healing consists of five stages: surface rearrangement, surface approach, wetting, diffusion and randomization [2]. The wetting stage responds to the crack tip recession. Fig. 4 shows a set of continuous pictures of the crack surface in the progressive healing of $\alpha = 0.5$ at 50°C. The time interval between two successive pictures is 30 s. It can be seen from Fig. 4 that the crack length L_c decreases linearly with increasing time. Yu et al. [3] assumed that chemical potential of the crack surface and healed zone near crack tip are proportional to the surface curvature and hydrostatic stress, respectively. The hydrostatic stress is proportional to the concentration of solvent, which is attributed to both Case I and Case II transport. Note that the solvent-induced stresses in polymer were derived by Wang et al. [35] in detail.

Table 4
The activation energies of a (E_a) and b (E_b) in Eq. (6)

α	0	0.2	0.3	0.4	0.5	0.6	0.7
E_a(kcal/mol.)	19.57	20.98	26.17	32.57	32.76	–	–
E_b(kcal/mol.)	7.01	8.99	10.73	13.14	15.57	17.57	19.57

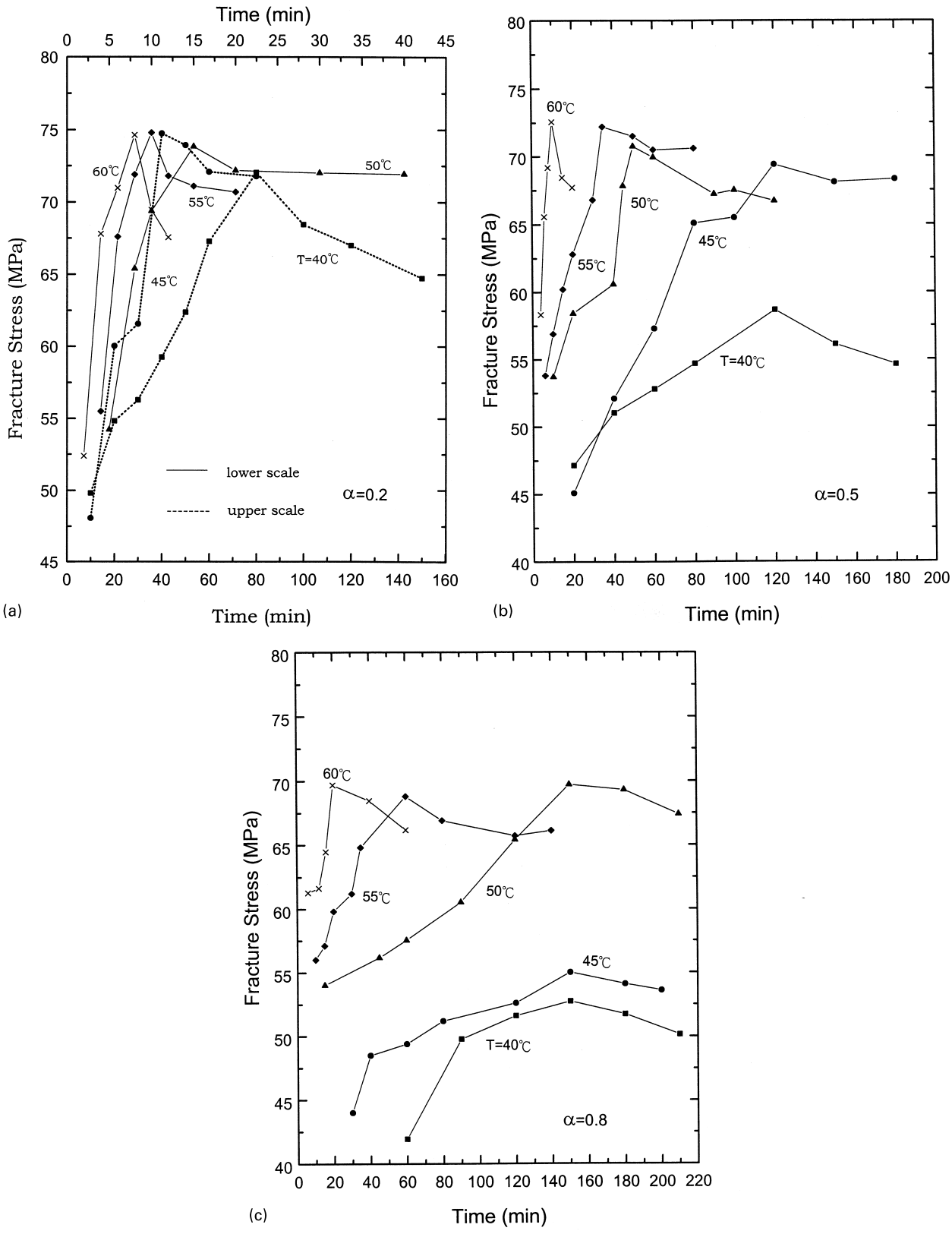

Fig. 5. The curves of fracture stress versus healing time: (a) $\alpha = 0.2$; (b) $\alpha = 0.5$ and (c) $\alpha = 0.8$.

Table 5
Crack closure rate V_H and the healing time t_H for different volume fractions of ethanol and temperatures

α	V_H, t_H	T (°C)				
		60	55	50	45	40
0	V_H (mm/sec)	0.1432	0.0841	0.0377	0.0188	0.0096
	t_H (sec)	44	75	167	335	656
0.2	V_H (mm/sec)	0.0997	0.0437	0.0222	0.0102	0.0049
	t_H (sec)	63	144	284	618	1286
0.5	V_H (mm/sec)	0.0521	0.0259	0.0141	0.0050	0.0022
	t_H (sec)	121	243	419	1260	2854
0.8	V_H (mm/sec)	0.0373	0.0175	0.0072	0.0023	0.0007
	t_H (sec)	169	359	871	2739	8439
1	V_H (mm/sec)	0.0158	0.0076	0.0028	0.0005	0.0002
	t_H (sec)	300	829	2223	11688	25727

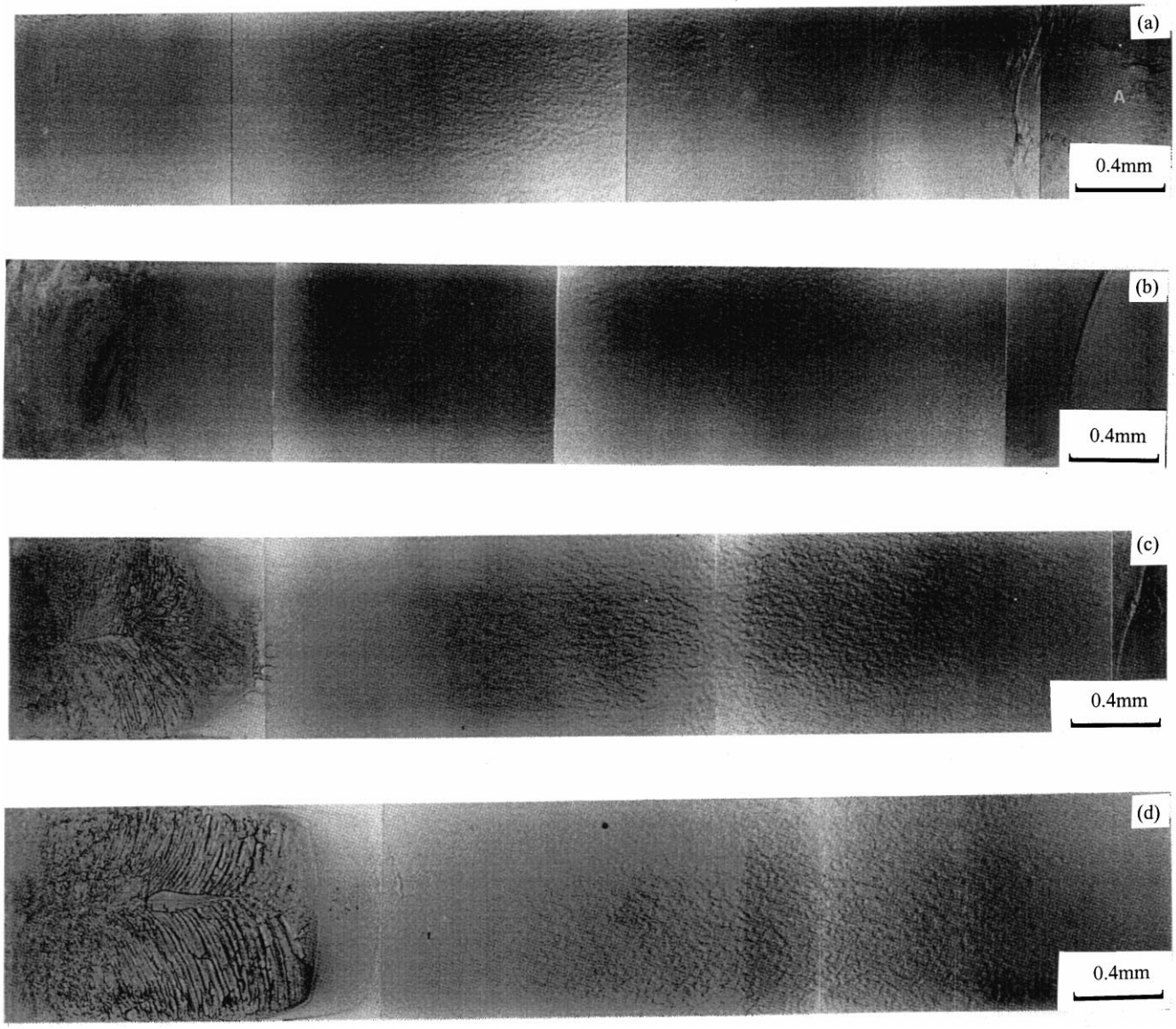

Fig. 6. Fractographies during crack tip recession, of PPMA treated with mixture of $\alpha = 0.5$ for periods of (a) 0 min, (b) 1 min, (c) 2 min, (d) 3 min, (e) 4 min, (f) 5 min, (g) 6 min, (h) 7 min, and (i) 8 min.

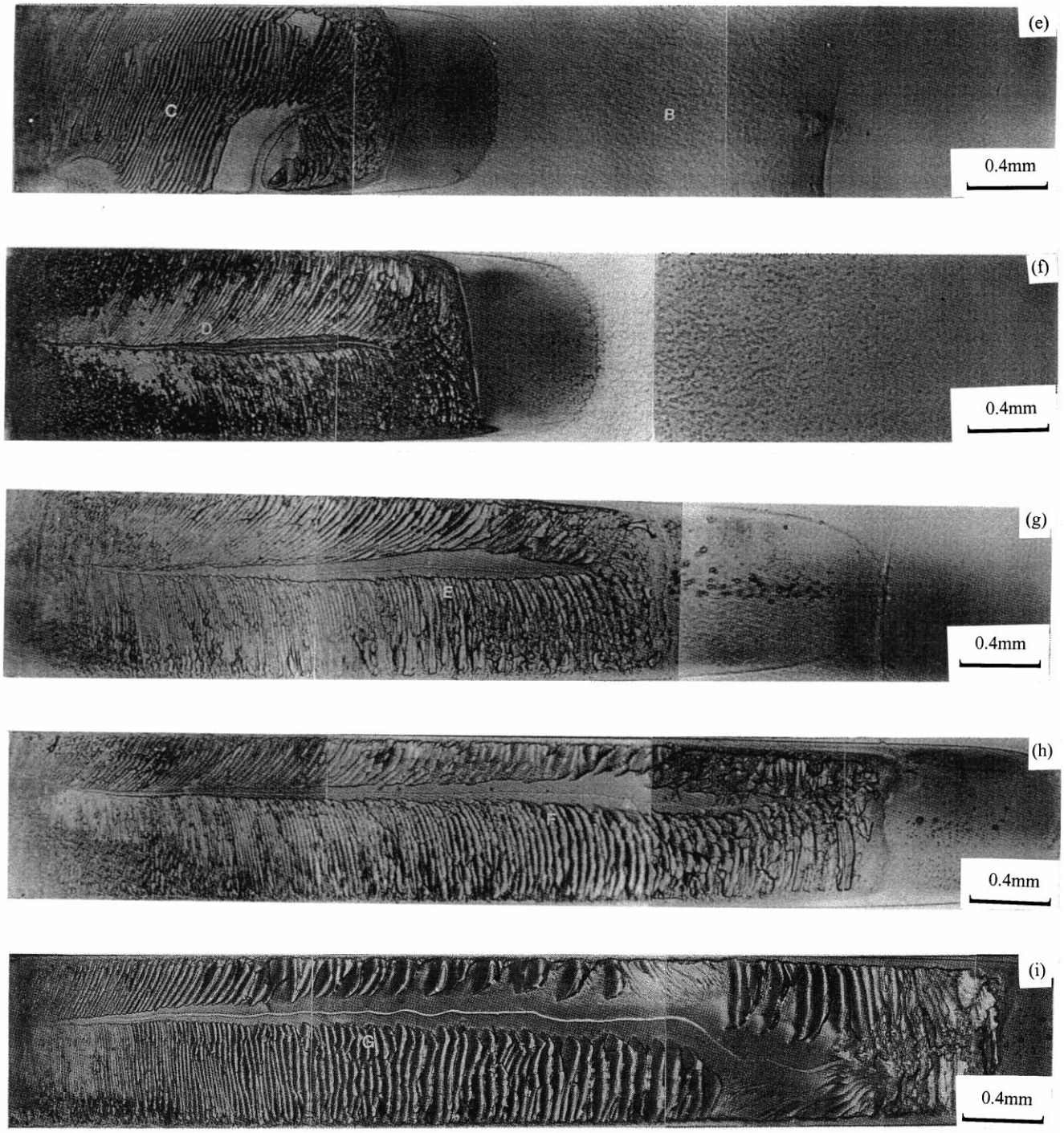

Fig. 6. (*continued*)

Then, based on the thermodynamics, Yu et al. obtained the crack length L_c during the wetting process as a function of time

$$L_c = L_0 - V_H t, \tag{7}$$

where L_0 and V_H are the original crack length and crack closure rate, respectively. V_H satisfies the modified Arrhenius' equation

$$V_H = \frac{V_H^0}{T} e^{-E_H/RT} \tag{8}$$

where V_H^D and E_H are the pre-exponent factor and activation energy. The crack closure rates for different volume fractions of ethanol and temperatures are listed in Table 5. The activation energy of crack closure is obtained from Table 5

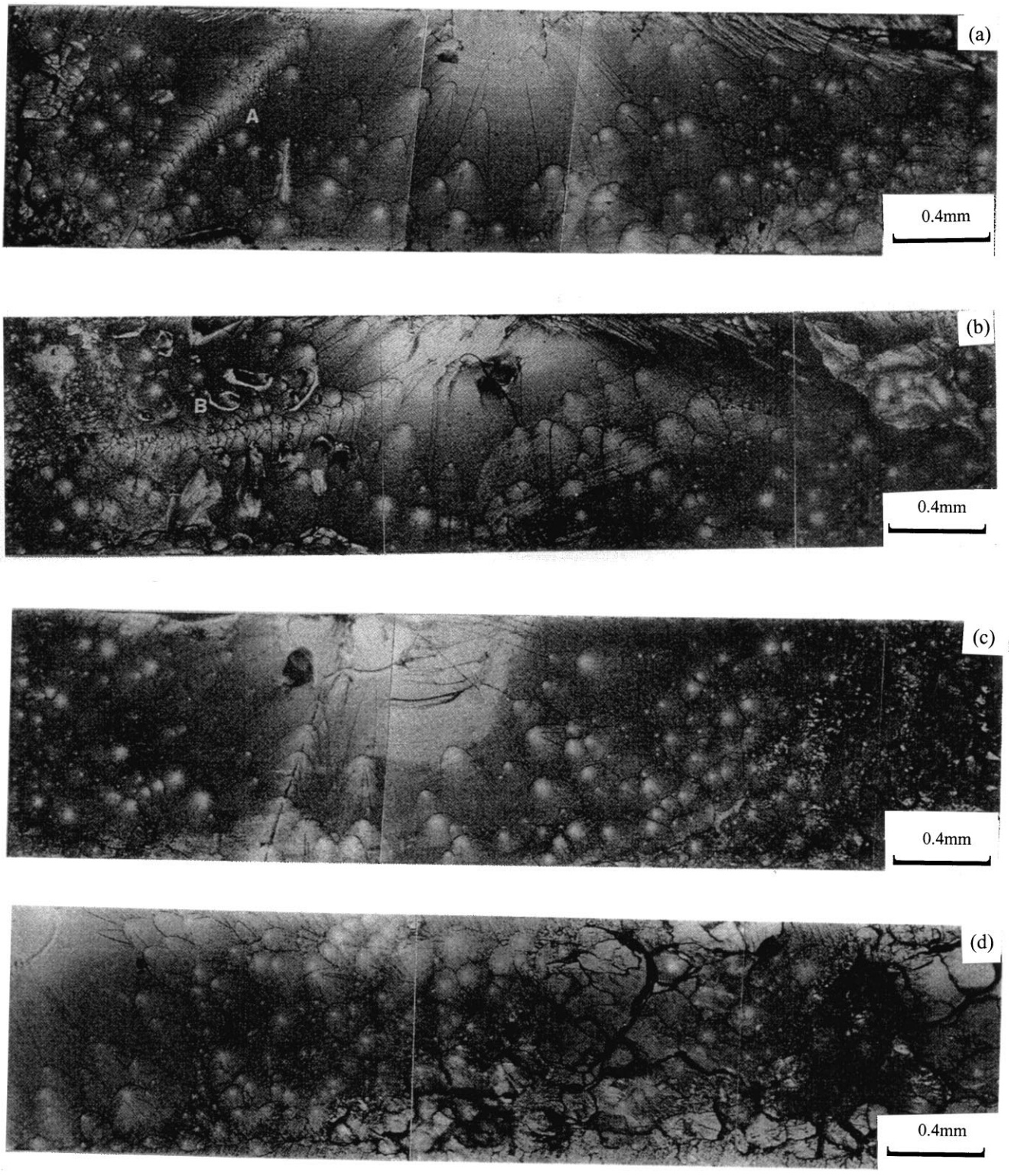

Fig. 7. Fractographies after the wetting stage, of PMMA treated with mixture of $\alpha = 0.5$ for periods of (a) 20 min, (b) 40 min, and (c) 50 min. (d) The fractograph of uncracked PPMA.

and Eq. (8) and listed in Table 2. It can be seen from Table 2 that the activation energy of crack closure is very close to that of Case II transport. That is, the crack closure is controlled by Case II transport.

3.4. Recovery of mechanical strength

During the crack tip recession (or wetting stage), the mechanical strength is very poor and unstable. After

wetting, the mechanical strength of cracked specimen recovers. That is, the diffusion stage is responsible for the strength of the healed specimen. The chains from one surface reptate into the region near the other surface and entangle with other chains. An external force is required to break the chain entanglement. Thus Fig. 5 shows the fracture stress σ_F versus the healing time at healing temperature 40–60°C, where the crack tip of specimen disappears. Note that the fracture stress of the uncracked specimen is 75 MPa. It can be seen from Fig. 5 that the fracture of PMMA for the same volume fraction of ethanol is better at a high healing temperature than at a low healing temperature. It is also found that the mechanical strength increases with decreasing α at the same healing temperature. When $\alpha \leq 0.2$, the mechanical strength can recover to the strength of the uncracked specimen. The fracture stress increases to a maximum and then decreases with increasing healing time. It is because the large amount of solvent creates polymer swelling. The relaxation of polymer chains at the cracked interface due to swelling makes the chains disentangle. The destruction region is frequently observed at the interface edge. It needs less time to reach maximum fracture stress with high healing temperatures and smaller α. The reason is that a large α is responsible for large swelling. The diffusion coefficient exponentially increases with temperature whereas penetration depth of chain increases with diffusion coefficient for a given time. The more the penetration depth is, the larger the fracture stress.

The self-diffusion of polymer chains occurs at the treated temperature above its effective glass transition temperature. The effective glass transition temperature is defined as the temperature to change from glassy state to rubber state of specimen treated with solvent. For DSC study, the effective glass transition temperature in this study is approximately equal to 20°C if the specimen is saturated with the mixture. That is, the treated temperature is greater than the effective glass transition temperature. Therefore, crack healing occurs at the temperature range 40–60°C.

3.5. Fractography

The morphology of fracture surfaces was observed. A set of continuous pictures in the wetting stage of healing process is shown in Fig. 6 where the specimen is treated with mixture of $\alpha = 0.5$ at 50°C. The original cleavage plane is shown in Fig. 6(a) where the crack is initiated at the region indicated by A and propagates toward the other end. Healing occurs at the crack tip and moves toward the region A. The cleavage surfaces affected by solvent are wetted and swollen, and then both surfaces approach each other to produce the crack closure. After crack closure, the polymer chains move from one surface to the other, and entangle with other polymer chains to recover the mechanical strength. Two features of fractography are observed; one feature corresponding to the unhealed zone indicated by B in Fig. 6(e) is featureless and the other corresponding to the healed region indicated by C in Fig. 6(e) shows many striations. The striation changes from fine to coarse as time increases. Two sets of striations are separated by lines indicated by D, E, F, and G in Fig. 6(f)–(i), respectively. The morphology of PMMA during crack tip recession is similar for all volume fractions of ethanol.

After completion of the wetting stage, the morphologies of the fracture surfaces were recorded at different healing times and are shown in Fig. 7. Many dimples toward the origin of fracture appear on the fracture surface. It is also found that continuous dimples indicated by A, B and C in Fig. 7(a)–(c), respectively, pile up, which was never observed on the fracture surface without solvent treatment. Comparing Figs. 6(a) and 7(d) for PMMA without solvent treatment, we find a plain feature on the cleavage plane and a lot of dimples on the fracture surface. After solvent treatment, a swollen zone forms near the crack surface. Interdiffusion of chains plays a role in swelling at the region near the crack interface and the greatest swelling is located at the crack edge, so that the crack edge is the most likely to be destroyed. The destruction region at the crack edge increases with increasing volume fraction of ethanol and exposure time. Thus the mechanical stress becomes small when the volume fraction of ethanol as well as the exposure time increase.

The fracture toughness in the interface [36] and fracture stress [37] are proportional to the healing time with exponent 1/4 during the isothermal healing. The polymer chain is mobile when its temperature is above the glass transition temperature. During the isothermal healing, both healing temperature and glass transition temperature are constant. That is, the difference between healing temperature and glass transition temperature is constant. However, the effective glass transition temperature during solvent healing decreases with increasing amount of solvent in polymer. Therefore, the diffusion coefficient of the polymer chain varies with healing time during the solvent healing. Wool and O'Connor [37] assumed that the fracture stress is proportional to penetration depth of the polymer chain. The penetration depth is proportional to the product of diffusion coefficient and diffusion time (or healing time). Therefore, it can be predicted that the fracture stress is not proportional to healing time with exponent 1/4 except that the healing temperature is very close to the glass transition temperature. It was fond that the exponent of the PMMA treated with pure methanol was close to 1/4 at healing temperature 40°C and less than 1/4 above 45°C [9]. In this experiment, the curves of fracture stress versus healing time shown in Fig. 5 cannot be fitted with a power law. The fracture stress increases to a maximum and then decreases with increasing healing time for $\alpha \geq 0.2$. The fracture stress at small healing times is controlled by self-diffusion of the polymer chain. The degradation at greater times is due to destruction of crack edge by swelling.

4. Summary and conclusions

Co-solvent of methanol and ethanol-induced crack healing in PMMA has been investigated. Solvent healing occurs when the effective glass transition temperature of PMMA is below the healing temperature. The crack tip recession is a linear function of healing time at a given solvent mixture and temperature. The crack closure rate satisfies the modified Arrhenius' equation. The fracture stress increases to a maximum and then decreases with increasing time. The increase of fracture stress is because the chains diffuse from one side to the other side and entangle with local chains. The reduction of fracture stress is due to dis-entanglement of polymer chains at the crack edge by swelling. The fracture stress increases with decreasing volume fraction of ethanol. Fractography provided evidence of crack healing. The crack tip recession is controlled by Case I transport.

The mass transport of solvent mixture in PMMA has also been studied. The mass transport of solvent mixture is anomalous, which is analyzed using Harmon's model. Harmon's model consists of Case I, Case II and anomalous transport. Both Case I and Case II transport satisfy Arrhenius' equation. Activation energies of Case I and Case II transport and heat of mixing are the average of activation energies of corresponding parameters of methanol and ethanol with a weighting factor based on the volume fraction. The solubility of solvent mixture is linearly proportional to the average of solubility of methanol and ethanol with a weighting factor based on the molecular weight. The sharp front is also studied. The sharp front position can be curved with $at^{1/2} + bt$. The activation energies of a and b are smaller than those of Case I and Case II transport, respectively. It is because the sharp front is controlled by the phase change from glassy state to rubber state and mass transport is controlled by atomic movement.

Acknowledgements

This work was supported by the National Science Council, Taiwan, Republic of China.

References

[1] Jud K, Kaush HH. Polym Bull 1979;1:697.
[2] Wool RP, O'Connor KM. J Appl Phys 1981;52:5953.
[3] Yu CC, Lin CB, Lee S. J Appl Phys 1995;78:212.
[4] Kim YH, Wool RP. Macromolecules 1983;16:1115.
[5] de Gennes PG. J Chem Phys 1971;55:572.
[6] Wool RP. ACS Polym Prepr 1982;23:62.
[7] Voyutski SS. In: Mark HF, Immergut EH, editors. Autohesion and adhesion of high polymers, Polym Rev, 4. New York: Wiley Interscience, 1963 (translated by Karganoff S from the original edited by Vakula VL).
[8] Wool RP. Polymer interface: structure and strength. New York: Hanser, 1995.
[9] Lin CB, Lee S, Liu KS. Polym Engng Sci 1990;30:1399.
[10] Wang PP, Lee S, Harmon JP. J Polym Sci, Part B: Polym Phys 1994;32: 1217.
[11] Kawagoe M, Nakanishi M, Qui J, Morita M. Polymer 1997;38:5969.
[12] Wu T, Lee S. J Polym Sci, Part B: Polym Phys 1994;32:2055.
[13] Alfrey T, Gurnee EF, Llyod WG. J Polym Sci, (C) 1966;12:249.
[14] Crank J. The mathematics of diffusion. 2nd ed. Oxford University Press, 1975.
[15] Thomas NL, Windle AH. Polymer 1978;19:255.
[16] Thomas NL, Windle AH. Polymer 1982;23:529.
[17] Hopfenberg MB, Nicolais L, Driode E. Polymer 1976;17:195.
[18] Friedman A, Rossi G. Macromolecules 1997;30:153.
[19] Govindjee S, Simo JC. J Mech Phys Solids 1993;41:863.
[20] Hui CY, Wu KC. J Appl Phys 1987;61:5129.
[21] Hui CY, Wu KC. J Appl Phys 1987;61:5137.
[22] Peterlin A. J Res Natl Bur Stand 1973;81:243.
[23] Wang TT, Kwei TK. Macromolecules 1973;6(6):919.
[24] Frisch HL, Wang TT, Kwei TK. J Polym Sci 1969;7(A-2):879.
[25] Wang TT, Kwei TK, Frisch HL. J Polym Sci 1969;7(A-2):2019.
[26] Kwei TK, Zupko HM. J Polym Sci 1969;7(A-2):867.
[27] Kwei TK, Wang TT, Zupko HM. Macromolecules 1969;5(5):867.
[28] Harmon JP, Lee S, Li JCM. J Polym Sci, Part A: Polym Chem 1987;25:3215.
[29] Harmon JP, Lee S, Li JCM. Polymer 1988;29:1221.
[30] Lee S. J Mater Res 1996;11:2407.
[31] Ouyang H, Lee S. J Mater Res 1996;11:2794.
[32] Ouyang H, Chen CC, Lee S, Yang H. J Polym Sci, Part B: Polym Phys 1998;36:163.
[33] Cowie JMG, Moshin MA, McEwen IJ. Polymer 1987;28:1569.
[34] Lin CB, Lee S, Liu KS. J Adhes 1991;34:221.
[35] Wang WL, Chen JR, Lee S. J Mater Res 1999;14:411.
[36] Jud K, Kausch HH, Williams JG. J Mater Sci 1981;16:204.
[37] Wool RP, O'Connor KM. J Polym Sci, Polym Lett Ed 1982;20:7.